

A DOUBLE WHITE-DWARF COOLING SEQUENCE IN ω CENTAURI*

A. Bellini¹, J. Anderson¹, M. Salaris², S. Cassisi³, L. R. Bedin⁴, G. Piotto^{5,4}, and P. Bergeron⁶
bellini@stsci.edu

Submitted on April 4, 2013, Accepted on May 1, 2013

Abstract

We have applied our empirical-PSF-based photometric techniques on a large number of calibration-related WFC3/UVIS UV-B exposures of the core of ω Cen, and found a well-defined split in the bright part of the white-dwarf cooling sequence (WDCS). The redder sequence is more populated by a factor of ~ 2 . We can explain the separation of the two sequences and their number ratio in terms of the He-normal and He-rich subpopulations that had been previously identified along the cluster main sequence. The blue WDCS is populated by the evolved stars of the He-normal component ($\sim 0.55 M_{\odot}$ CO-core DA objects) while the red WDCS hosts the end-products of the He-rich population ($\sim 0.46 M_{\odot}$ objects, $\sim 10\%$ CO-core and $\sim 90\%$ He-core WDs). The He-core WDs correspond to He-rich stars that missed the central He-ignition, and we estimate their fraction by analyzing the population ratios along the cluster horizontal branch.

Subject headings: globular clusters: individual (NGC 5139) — Hertzsprung-Russell and C-M diagrams — stars: Population II — white dwarfs — techniques: photometric

1. Introduction

The massive globular cluster (GC) ω Cen has been studied since the ‘60s because of its peculiar stellar populations (see van Leeuwen, Hughes & Piotto 2002 for a review). The discovery of its multiple stellar generations (Bedin et al. 2004, Bellini et al. 2010) has further revitalized detailed photometric and spectroscopic investigations of this object. The white-dwarf (WD) cooling sequence (CS) is the least-studied part of the color-magnitude diagram (CMD) of this cluster, for the obvious reason that WDs are faint and are usually concentrated in the most-crowded central regions.

Ortolani & Rosino (1987) were the first to detect a dozen WDs in ω Cen, but it is only with the advent of *HST* that it became possible to analyze the WDCS in more detail (Monelli et al. 2005; Calamida et al. 2008). In particular, Calamida

et al. showed that the WDCS spread in color is larger than expected from photometric errors alone. We will show here that the WDCS of ω Cen actually splits into *two distinct sequences*, which can be explained as separate WD populations of different mass and chemical stratification, corresponding to the evolved components of the separate subpopulations with differing helium abundances, as revealed by the photometric analysis of main-sequence stars (e.g. King et al. 2012 and references therein).

2. Data sets and reduction

This analysis is based on *HST*’s WFC3/UVIS observations taken between 2009 and 2011 under WFC3 calibration programs. Specifically: we have 27×900 s exposures in F225W, 31×800 s in F275W, 37×350 s in F336W, and 34×350 s in F438W. The field of view (FoV) is centered on the cluster’s center, and covers the inner $\sim 150''$.

All WFC3/UVIS *_flt* images for a given filter were analyzed simultaneously to generate an astrometric and photometric catalog of stars in the field, using an evolution of the software tools described in Anderson et al. (2008). Briefly, we used information from all the available exposures for a given filter to find significant detections across the FoV. These detections were then fit independently in each exposure by employing a fixed array of 7×8 spatially-varying static library PSF models, plus a 5×5 array of perturbation PSFs tailored to fit the star profiles in each exposure in order to account for focus/breathing variations. Positions were corrected for geometric distortion according to the routines in Bellini, Anderson & Bedin (2011). The photometry was calibrated into the

¹Space Telescope Science Institute, 3700 San Martin Dr., Baltimore, MD 21218, USA

²Astrophysics Research Institute, Liverpool John Moores University, Twelve Quays House, Egerton Wharf, Birkenhead, CH41 1LD, United Kingdom

³Istituto Nazionale di Astrofisica, Osservatorio Astronomico di Collurania, via Mentore Maggini, I-64100 Teramo, Italy

⁴Istituto Nazionale di Astrofisica, Osservatorio Astronomico di Padova, v.co dell’Osservatorio 5, I-35122, Padova, Italy

⁵Dipartimento di Fisica e Astronomia “Galileo Galilei”, Università di Padova, v.co dell’Osservatorio 3, I-35122, Padova, Italy

⁶Département de Physique, Université de Montréal, C.P. 6128, Succ. Centre-Ville, Montréal, Québec H3C 3J7, Canada

*Based on archival observations with the NASA/ESA *Hubble Space Telescope*, obtained at the Space Telescope Science Institute, which is operated by AURA, Inc., under NASA contract NAS 5-26555.

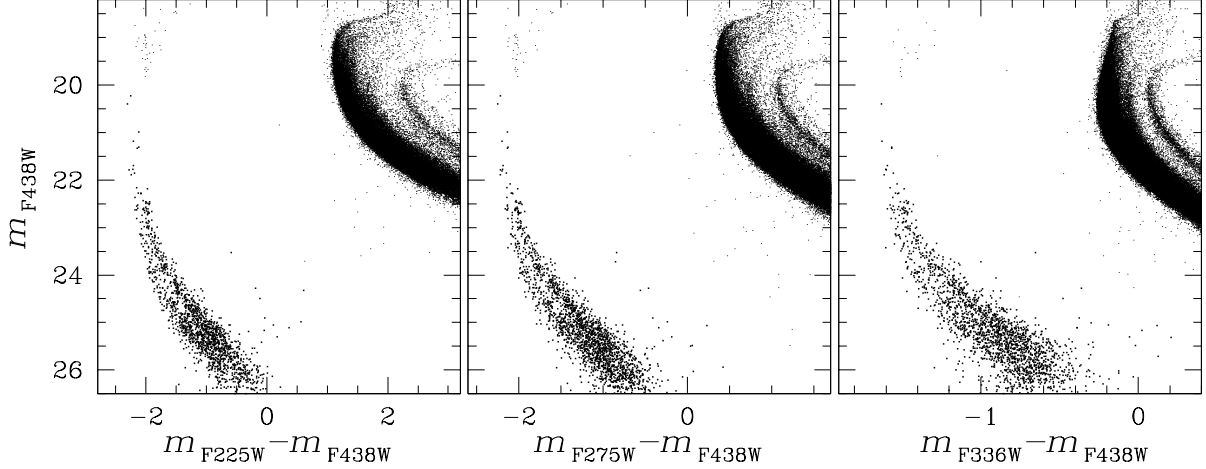


Fig. 1.— The double WDCS of ω Cen: from left to right we show m_{F438W} versus $m_{F225W} - m_{F438W}$, $m_{F275W} - m_{F438W}$, and $m_{F336W} - m_{F438W}$, respectively.

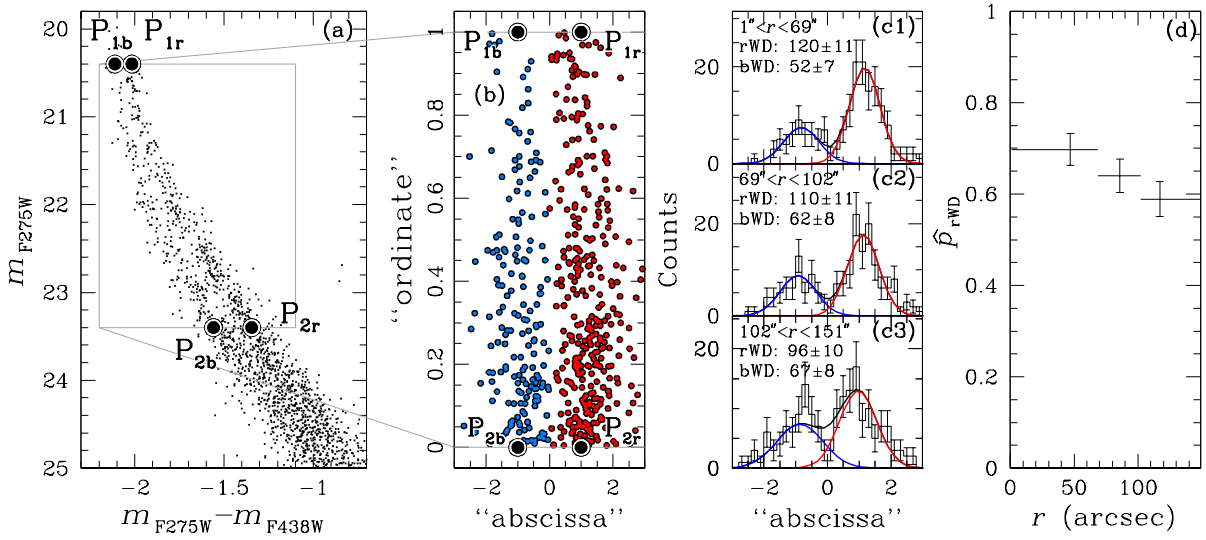


Fig. 2.— (a) Blow-up of the WDCS in the m_{F275W} versus $m_{F275W} - m_{F438W}$ CMD with the four points used in the coordinate-system transformation of the next panel. (b) Rectification of the WDCS region that was shown in gray in panel (a). Here we define as bWD (in blue) those stars having “abscissa” < 0 , rWD stars the others (in red). (c) The FoV is divided into three equally-populated radial intervals. For each of them we fit a dual Gaussian to the “abscissa” distribution, and used the area of the two Gaussians to estimate the number of bWD and rWD stars in each radial interval (radial extension and areas are quoted in each panel). (d) Radial distribution of the ratio of rWD with respect to the total WD population.

Vega-mag flight system following Bedin et al. (2005), using the WFC3 zero points provided by the STScI¹.

3. The Double WD CS

Figure 1 shows the WDCS of ω Cen in three different CMDs, keeping the m_{F438W} magnitude on the vertical axis, and using a variety of color combinations. WDs are shown with heavier dots, for clarity. We identified over 2,000 WDs across the FoV. The WDCS can be followed for over 6 magnitudes in m_{F438W} , starting from just below the termination point of the

extreme horizontal branch (HB). Two distinct and well defined WD sequences are visible in the bright part of the CS, before becoming indistinguishable below $m_{F438W} \sim 25$. A few stars, about 1 magnitude redder than the WDCS, define an additional, scarcely populated sequence.

Stars on the main sequence (MS) of ω Cen are well known to be separated into three main components: (1) a He-rich bMS, (2) a He-normal, [Fe/H]-poor rMS, and (3) a [Fe/H]-rich MS-a (Anderson 1997; Bedin et al. 2004; Piotto et al. 2005; Bellini et al. 2010). The bMS has been found to be more centrally concentrated than the rMS (Sollima et al. 2007; Bellini et al. 2009), a fossil signature of the formation process of the two populations. Indeed, the present-day relaxation time

¹http://www.stsci.edu/hst/wfc3/phot_zp_1bn.

($t_{\text{relax}} = 12.3$ Gyr, Harris 1996, 2010 edition) suggests the two populations have not yet had enough time to mix.

In order to look for a connection between the split WDCS and the split MS, we measured the radial distribution of the two WD components as follows. We started by selecting stars in the $m_{\text{F275W}} - m_{\text{F438W}}$ CMD (Figure 2a). To optimally separate the populations, we used a procedure developed by Milone et al. (2009). We first selected by hand two points (P_{1b}, P_{2b}) on the blue CS, and two points (P_{1r}, P_{2r}) on the red one. We then linearly transformed the CMD into a reference frame in which the coordinates of P_{1b} , P_{2b} , P_{1r} , and P_{2r} , map to $(-1,1)$, $(-1,0)$, $(1,1)$ and $(1,0)$, respectively (Figure 2b). Here the blue component (the bWD) maps to negative “abscissa” values, and the red component (the rWD) to positive “abscissa” values (color coded in blue and red, respectively, in panel (b)). To examine the radial distribution we followed the methods by Bellini et al. (2013). We divided the FoV into three equally-populated radial intervals, and fit in each of them a Gaussian to each of the color-like distribution of bWD and rWD stars (panels (c)). (A dual-Gaussian fit is more robust than simply adding up stars in histogram bins.) The radial coverage of interest and the areas of each of the two Gaussians are given in the top-left corner of each of these panels. Panel (d) shows the quantity $\hat{p}_{\text{rWD}} = N_{\text{rWD}}/(N_{\text{rWD}} + N_{\text{bWD}})$ as a function of distance from the cluster center. Binomial errors are $\sim 3.7\%$. There is marginal evidence for a gradient, with rWD stars more concentrated than bWD ones. Moreover, rWD stars (326) are $\sim 64\%$ of the total bWD+rWD stars (507). We note that Bellini et al. (2010) also did not find any strong evidence of a radial gradient in the ratio of the two main MSs in the inner 2 arcmin of ω Cen (see their Fig. 18).

The top and middle panels of Fig. 3 show the WDCS CMD in a wide variety of color systems, with the same stars color-coded the same ways in all the panels. The split is present in all of them. It is interesting to note, however, that even though all the other populations (MS, sub-giant branch, etc) show dramatic splits in two-color diagrams (2CDs), there is *no* split in the 2CDs plotted in the bottom panels of Fig. 3. This implies that the split is likely due to a discrete mass/radius difference between the populations, rather than an atmospheric effect.

4. The nature of the two WDSCs

We have adopted the distance modulus derived from the cluster eclipsing binary OGLEGC 17 (Thompson et al. 2001), i.e., $(m - M)_0 = 13.66 \pm 0.12$, and a mean value of the reddening $E(B - V) = 0.12$ as in King et al. (2012). To calculate the extinction in our filters we have applied the extinction law of Cardelli et al. (1989, with $R_V = 3.1$) to our WD spectra used for the calculation of the bolometric corrections to the UVIS filters². The resulting extinctions in the F275W, F438W and F336W filters are: 0.75, 0.50 and 0.62 mag, respectively. These values were applied to our WD tracks –

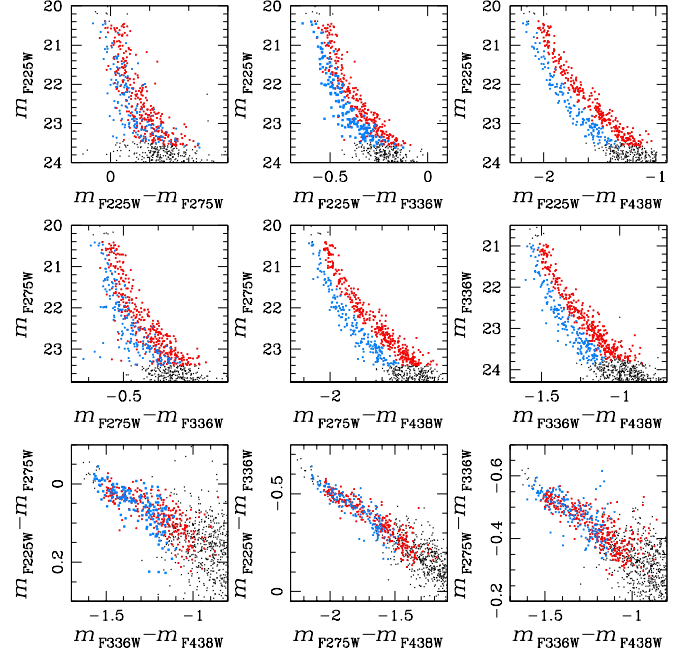


Fig. 3.— *Top and middle panels*: multicolor analysis for the WDSC. *Bottom panels*: two-color diagrams. Red and blue WDs are those defined in Figure 2b.

transformed to the UVIS filters – from BaSTI CO-core WD models by Salaris et al. (2010), He-core tracks by Bedin et al. (2008a) and Serenelli et al. (2002), and additional CO-core models calculated specifically for this project. We focus here on the m_{F275W} versus $m_{\text{F275W}} - m_{\text{F438W}}$ CMD, which shows a very clear separation of the two WDSCs.

The brightest few magnitudes of a WDSC are populated by objects that just entered the cooling sequence and are therefore cooling extremely rapidly. We can thus approximate all the stars in this transient stage as having the same WD mass, since they presumably all started with the same turnoff (TO) mass. It is therefore also safe to match them with single-mass cooling tracks rather than formal WD isochrones. Theory predicts a typical WD mass of $\sim 0.54 M_{\odot}$ in old populations (see, e.g., Weiss & Ferguson 2009), which is consistent with what Kalirai et al. (2004) found in a spectroscopic study of six bright DA WDs in M 4.

There are a few possible theoretical explanations for the split of the bright WDSC of ω Cen: (1) unresolved WD+WD binaries, (2) a combination of DA+DB objects, or (3) bimodal WD mass distribution, presumably related to the He-enhanced subpopulation.

Regarding the binary scenario, we note that the split WDSC at these bright magnitudes cannot be explained by unresolved $\sim 0.54 M_{\odot}$ WD+WD binaries. Although the split we observe is very nearly equal to that expected for equal-mass binaries, the masses of the two components would have to be nearly identical at birth, since only an extremely narrow range of initial

²<http://www.astro.umontreal.ca/~bergeron/CoolingModels>.

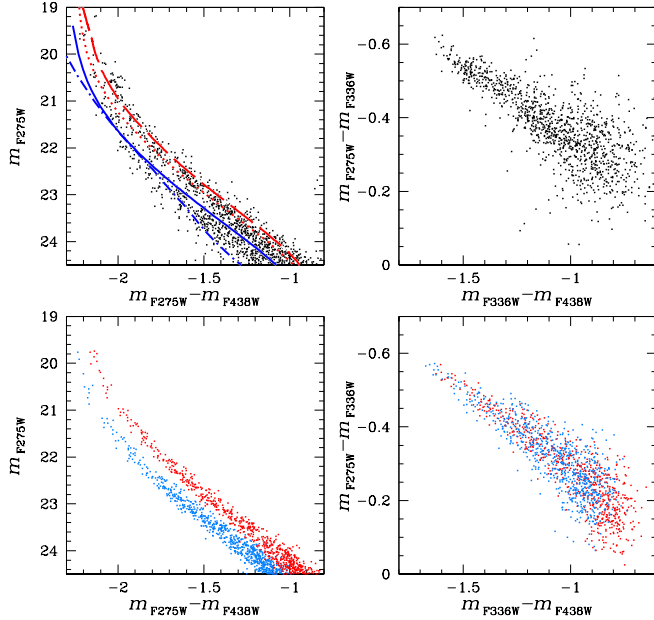


Fig. 4.— *Left panels*: one of the observed CMDs of Fig. 3 (top) and a theoretical counterpart (bottom). WD tracks for CO-core $0.55M_{\odot}$ DA (blue solid) and DB models (blue dash-dotted), $0.46M_{\odot}$ DA CO-core (red dotted) and He-core (red dashed) models are fit to the observed CMD. In the theoretical panels, stars are color coded in azure ($0.55M_{\odot}$) and red ($0.46M_{\odot}$). *Right panels*: one of the observed 2CDs of Fig. 3 (top) and a theoretical counterpart (bottom).

mass occupies the transient cooling phase at the same time. If the mass ratio of the progenitors is distributed approximately homogeneously between 0 and 1 (as found by Milone et al. 2012), then the two components would be continuously distributed over a large magnitude range, and the net effect would be a moderate widening of the bright WDCS, not a split (as shown for example by the simulations for NGC 6791, Bedin et al. 2008b).

We now explore the possibilities that the split is caused by either a combination of DA+DB objects or a WD mass dichotomy. The top-left panel of Fig. 4 superposes on the observed WDSCS four theoretical cooling sequences: a $0.55M_{\odot}$ CO-core DA track (blue solid line), the DB counterpart (blue dash-dotted line), a $0.46M_{\odot}$ CO-core DA track (red dotted line), and a He-core track (and DA atmosphere) with the same $0.46M_{\odot}$ mass (red dashed line).

The $0.55M_{\odot}$ DA model that fits the bWD sequence for the eclipsing binary distance represents the “canonical” WD population. The DB track for the same mass is very close to the DA track in the region of interest, so the split cannot be explained by DA and DB populations with the same mass. We note that a bimodal H-layer mass distribution is also ruled out because any sequence with lower thickness (the “standard” value $10^{-4}M_{\text{WD}}$ employed in our models is an upper evolutionary limit) is shifted to bluer colors and cannot explain the red sequence.

The only explanation for the rWD objects is therefore a sequence of lower-mass WDs, which would consequently have larger radii. We find that the rWD sequence can be reproduced by $\sim 0.46M_{\odot}$ models, with either CO- or He-cores.

The bottom left-hand panel of Fig. 4 shows a CMD obtained from a composite synthetic sample made of the $0.55M_{\odot}$ DA and $\sim 0.46M_{\odot}$ He-core models. The photometric error has been implemented following the results of the data reduction. The synthetic CMD reproduces the bright split sequence, which in the simulation merges around $m_{\text{F275W}} \sim 23.5$ —consistent with the observations—due to the increased photometric error. The right-hand panels of Fig. 4 show one of the 2CDs of Fig. 3, both observed (top) and simulated (bottom). Notice that, like the observations, the simulated sample also does not show the bWD+rWD split in the color-color plane.

5. The Origin of the rWD Sequence

It is tempting to map the two WD populations to the two main MS components, and associate the rWD sequence with the helium-rich MS population. To test this hypothesis, we can also use the ratio of bWD to rWD stars, and compare it with theoretical predictions. First of all, we need to know what kind of WDs each is made up of, since CO and He WDs cool at different rates. An answer to these questions requires a brief examination of the cluster HB morphology.

Cassisi et al. (2009, C09) showed that the progeny of the He-enhanced MS ($Y = 0.40$) must be confined to the blue tail of the observed HB, and found that the blue clump of stars at the end of the extended HB tail (see Fig. 2 of C09) can be reproduced by either hot flashers or canonical He-rich HB stars, or a mixture of both types.

The minimum mass for the He-rich component along the HB is $\sim 0.46M_{\odot}$ (C09). These objects will form CO-core WDs with essentially the same mass. Even a small amount of additional mass loss along the red giant branch (RGB) would prevent core He-ignition and produce $\sim 0.46M_{\odot}$ He-core WDs. Note that these stars with high initial He abundances need to lose only $\sim 0.10\text{--}0.15 M_{\odot}$ along the RGB to fall below the limit for He-ignition, since their TO mass is about $\sim 0.2M_{\odot}$ less than that of the normal-He stars.

The presence of the “mass gap” between the two WD sequences (0.55 vs. $0.46 M_{\odot}$) supports the idea that the blue clump in the HB is populated mainly by the evolved members of the He-rich subpopulation, which eventually become CO and—possibly—He-core WDs with a mass of $\sim 0.46M_{\odot}$, creating the rWD sequence. On the other hand, the bWD sequence is instead produced by the end-products of He-normal stars ($Y = 0.25$) that populate the rest of the observed HB. Although a fraction of the He-normal population *could* explain the red end of the blue clump, such stars would have $\sim 0.49M_{\odot}$ cores and the resulting WDs, with essentially the same mass (because of the vanishingly small envelopes of their HB progenitors), would occupy the gap between the observed

sequences.

With this understanding of the evolutionary origin of the rWD sequence, we investigate whether our interpretation can also explain the observed $N_{\text{rWD}}/N_{\text{bWD}} = 1.8 \pm 0.2$ number ratio in the magnitude range $20.4 < m_{\text{F275W}} < 23.4$. Our CMDs show that the ratio between blue-clump stars and the rest of the HB population is ~ 0.32 , and the ratio between the He-normal and He-rich populations along the MS is ~ 1 in this central field.

We consider two 13.5 Gyr isochrones from the BaSTI database (Pietrinferni et al. 2006): one with $[\text{Fe}/\text{H}] = -1.6$, $Y = 0.246$ to represent the He-normal population, and the other with $[\text{Fe}/\text{H}] = -1.3$, $Y = 0.40$ to represent the He-rich component. The exact age is not critical: if the age of both components is decreased by 1-2 Gyr and/or the He-rich population is made younger by ~ 1 Gyr, the quantitative result of our analysis is largely unchanged. The isochrones allow us to calculate the so-called *evolutionary flux*, which tells us the number of stars leaving the MS per year:

$$b(t) = \Phi(M_{\text{TO}}) \left| \frac{d}{dt} M_{\text{TO}} \right| = A \times M_{\text{TO}}^{-2.3} \left| \frac{d}{dt} M_{\text{TO}} \right|$$

(Renzini & Buzzoni 1986). The adopted mass function $\Phi(M_{\text{TO}})$ has the Salpeter slope. The TO mass M_{TO} and its time-derivative are determined from the isochrones, and the constant A is fixed by constraining that the number of MS stars (below the TO) of the two components to be the same. (Note that the MS is the only region that allows us to determine the mass-function normalization and initial fraction of He-rich stars). The value of $b(t)$ of the He-enhanced population turns out to be 1.1 times the value for the He-normal component. Given that beyond the TO (apart from the faint end of the WDCS) the initial value of the evolving mass along an isochrone is $\sim M_{\text{TO}}$, the number of stars in a given post-MS phase can be approximated by $N_{\text{PMS}} = b(t) \times t_{\text{PMS}}$ (where t_{PMS} is the lifetime of the post-MS evolutionary stage).

The typical HB mass for stars in the He-normal component (i.e., not in the blue clump) is $\sim 0.61\text{--}0.62 M_{\odot}$. Using $b(t)$, the model HB timescales provide an expected number ratio of ~ 1.7 between blue-clump stars (He-rich) and the rest of the HB population. The observed ratio is ~ 0.32 , thus only $\sim 20\%$ of the He-rich population must have produced blue-clump stars. This means that $\sim 80\%$ of the He-burning stars that we expect from the He-rich component seen along the MS, must have missed the He-ignition and evolved onto the WDCS, as He-core WDs. If these stars left the RGB close to He-ignition (where mass loss is expected to be more efficient), they now populate the rWD sequence as $\sim 0.46 M_{\odot}$ He-core WDs. Likewise, the progeny on the (He-rich) HB blue clump produced $\sim 0.46 M_{\odot}$ CO-core WDs, and the He-normal population produced “canonical” $0.55 M_{\odot}$ CO-core WDs.

We can now split the *evolutionary flux* for the He-rich population into two components, according to the fraction of stars that achieve He-ignition. Over the magnitude range of interest,

the $0.46 M_{\odot}$ CO-core model has approximately the same cooling time of the $0.55 M_{\odot}$ model (on the order of 10^8 yrs), while the $0.46 M_{\odot}$ He-core model has cooling timescales a factor of ~ 2.4 longer. By considering these $b(t)$ and timescale ratios, we derive an expected number ratio:

$$\frac{N_{\text{rWD}}}{N_{\text{bWD}}} = \frac{b(\text{prog. rWD})^{\text{He core}} \times t_{\text{rWD}}^{\text{He core}}}{b(\text{prog. bWD}) \times t_{\text{bWD}}} + \frac{b(\text{prog. rWD})^{\text{CO core}} \times t_{\text{rWD}}^{\text{CO core}}}{b(\text{prog. bWD}) \times t_{\text{bWD}}}$$

and, since $t_{\text{rWD}}^{\text{He core}}/t_{\text{bWD}} = 2.4$ and $t_{\text{rWD}}^{\text{CO core}}/t_{\text{bWD}} = 1.0$, we have

$$\frac{N_{\text{rWD}}}{N_{\text{bWD}}} \simeq 0.8 \times 1.1 \times 2.4 + 0.2 \times 1.1 \times 1.0 \simeq 2.3,$$

not far from the observed value of 1.8 ± 0.2 . This also implies that the number of He-core WDs along the rWD sequence is $\simeq (0.8 \times 1.1 \times 2.4)/(0.2 \times 1.1 \times 1.0) \simeq 10$ times the number of CO-core WDs.

To summarize, when taking into account the various evolutionary paths during the post-MS phases of the He-rich and He-normal MS components and the appropriate timescales, we can reasonably reproduce the observed $N_{\text{rWD}}/N_{\text{bWD}}$ ratio, and derive a very high fraction of He-core WDs along the red CS.

6. Summary and Conclusions

Our high-precision, empirical-PSF-based photometric techniques have revealed a never-before-seen split in the bright part of the WDCS in a Galactic GC. We have interpreted the observed WDCS as follows:

- The blue sequence corresponds to $\sim 0.55 M_{\odot}$ CO-core WDs from the He-normal MS population, and the red sequence corresponds to $\sim 0.46 M_{\odot}$ both CO-core and He-core WDs from the He-enriched population. The radial gradients of the various populations are consistent with this scenario.
- The “mass gap” between the two WD sequences means that the blue clump along the cluster HB has to be populated mainly by stars belonging to the He-rich component.
- The observed number ratio between blue-clump HB stars and the rest of the HB population is consistent with the number ratio of He-rich to He-normal MS stars, only if $\sim 80\%$ of the HB stars expected to be produced by the He-rich component failed to achieve He-ignition and evolved onto the red WDCS as $\sim 0.46 M_{\odot}$ He-core WDs.
- It is *not* extreme mass loss that produces these He-core WDs, but rather the fact that the TO mass of the He-rich subpopulation is $\sim 0.2 M_{\odot}$ lower than that of the He-normal component. A total mass loss of just $\sim 0.15 M_{\odot}$

along the RGB suffices to prevent central He-ignition for this subpopulation.

- The number ratio between CO-core and He-core WDs (with longer cooling times) along the red WDCS is ~ 0.1 . This mixture of WDs along the red WDCS approximately explains the observed number ratio (rWD/bWD). This large contribution of massive He-core WDs confirms the more indirect inference by Calamida et al. (2008), that the bright WD sequence must be populated by a substantial fraction of He-core WDs.

In conclusion, our observations and theoretical analysis have for the first time disclosed a connection between globular clusters with extreme blue HB stars and enhanced He, and the morphology – hence mass distribution – of their WDCS. It would be extremely important to study the bright WDCS in other clusters with extreme HBs and He-rich subpopulations (i.e. NGC 6752, NGC 2808) to see whether a split WDCS analogous to the one detected in ω Cen can be found.

Acknowledgments. AB and JA acknowledge support from STScI grant AR-12656. GP acknowledges partial support by the Università degli Studi di Padova CPDA101477 grant.

REFERENCES

- Anderson, J., Ph.D. thesis, Univ. of California, Berkeley, 1997
- Anderson, J. et al. 2008, *AJ*, 135, 2055
- Bedin, L. R., Piotto, G., Anderson, J., et al. 2004, *ApJ*, 605, L125
- Bedin, L. R., Cassisi, S., Castelli, F. et al. 2005, *MNRAS*, 357, 1038
- Bedin, L.R., King, I.R., Anderson, J., Piotto, G., Salaris, M., Cassisi, S., & Serenelli, A. 2008a, *ApJ*, 678, 1279
- Bedin, L.R., Salaris, M., Piotto, G., Cassisi, S., Milone, A.P., Anderson, J., & King, I.R. 2008b, *ApJ*, 679, 29
- Bellini, A., Piotto, G., Bedin, L. R., et al. 2009, *A&A*, 507, 1393
- Bellini, A., Bedin, L. R., Piotto, G., et al. 2010, *AJ*, 140, 631
- Bellini, A., Anderson, J., & Bedin, L. R. 2011, *PASP*, 123, 622
- Bellini, A., Piotto, G., Milone, A. P., et al. 2013, *ApJ*, 765, 32
- Calamida, A., Corsi, C. E., Bono, G., et al. 2008, *ApJ*, 673, L29
- Cassisi, S., Salaris, M., Anderson, J., et al. 2009, *ApJ*, 702, 1530 (C09)
- Cardelli, J. A., Clayton, G. C., & Mathis, J. S. 1989, *ApJ*, 345, 245
- Harris, W.E. 1996, *AJ*, 112, 1487
- Kalirai, J. S., Saul Davis, D., Richer, H. B., et al. 2009, *ApJ*, 705, 408
- King, I.R., Bedin, L.R., Cassisi, S., Milone, A.P., Bellini, A., Piotto, G., Anderson, J., Pietrinferni, A., & Cordier, D. 2012, *AJ*, 144, 5
- Milone, A. P., Stetson, P. B., Piotto, G., et al. 2009, *A&A*, 503, 755
- Milone, A. P., Piotto, G., Bedin, L. R., et al. 2012, *A&A*, 540, A16
- Monelli, M., Corsi, C. E., Castellani, V., et al. 2005, *ApJ*, 621, L117
- Ortolani, S., & Rosino, L. 1987, *A&A*, 185, 102
- Pietrinferni, A., Cassisi, S., Salaris, M., & Castelli, F. 2006, *ApJ*, 642, 797
- Piotto, G., Villanova, S., Bedin, L. R., et al. 2005, *ApJ*, 621, 777
- Renzini, A., & Buzzoni, A. 1986, in *Spectral Evolution of Galaxies, Astrophysics and Space Science Library*, Chiosi, C. and Renzini, A. Eds., p.195
- Salaris, M., Cassisi, S., Pietrinferni, A., Kowalski, P.M., & Isern, J. 2010, *ApJ*, 716, 1241
- Serenelli A. M., Althaus L. G., Rohrmann R. D., et al. 2002, *MNRAS*, 337, 1091
- Sollima, A., Ferraro, F. R., Bellazzini, M., Origlia, L., Straniero, O., & Pancino, E. 2007, *ApJ*, 654, 915
- Thompson, I.B., Kaluzny, J., Pych, W. et al. 2001, *AJ*, 121, 3089
- van Leeuwen, F., Hughes, J. D., & Piotto, G. 2002, *Omega Centauri, A Unique Window into Astrophysics*, 265
- Weiss, A., & Ferguson, J.W. 2009, *A&A*, 508, 1343